Proximity effects in an exchange-biased $Ni_{80}Fe_{20}/Co_3O_4$ thin film

J. van Lierop,[1] K.-W. Lin,[2] J.-Y. Guo,[2] H. Ouyang,[2] and B. W. Southern[1]
[1]*Department of Physics and Astronomy, University of Manitoba, Winnipeg MB, R3T 2N2, Canada*
[2]*Department of Materials Engineering, National Chung Hsing University, Taichung 402, Taiwan*
(Received 14 December 2006; published 12 April 2007)

An unusual enhancement of the antiferromagnetic ordering (Néel) temperature is observed in a $Ni_{80}Fe_{20}/Co_3O_4$ thin film. This significant increase of the Néel temperature indicates an exchange energy of interface spins between the ferromagnet (FM) and antiferromagnet (AF) that is significantly greater than that of spins in the bulk of the film. Exchange bias is established even when the thin film is zero field cooled. Field cooling the film sets a significantly stronger exchange coupling between the FM and AF spins at the interface with a concomitant increase in the exchange-bias field.

DOI: 10.1103/PhysRevB.75.134409 PACS number(s): 75.30.Et, 75.70.Cn, 75.75.+a

I. INTRODUCTION

Nanomagnetism is at the forefront of magnetic research and is motivated by seeking a fundamental understanding of the physics as well as by technological applications. A major challenge in nanomagnetism is understanding exchange bias, which is of significant importance to magnetic media. In thin-film bilayers composed of a ferromagnetic (FM) and an antiferromagnetic (AF) layer, a unidirectional anisotropy occurs when spins at the interface of AF and FM layers couple.[1–3] This unidirectional anisotropy alters the basic magnetism of the combined AF/FM system and results in a distinctive shift of a hysteresis loop away from zero along the magnetic-field axis. The exchange bias field H_{ex} represents this loop shift and is an outcome of the unidirectional anisotropy. During the measurement of a hysteresis loop, the resulting torque on the ferromagnetic moments creates the exchange bias loop shift in addition to an enhanced coercivity H_c compared to the pure FM film. A fundamental understanding of H_{ex} and H_c is important for device applications.

Even though the circumstances that give rise to exchange bias are understood, the basic mechanism remains unclear. Central to the physics of exchange bias is the temperature dependence of the interfacial coupling that affects both the measured H_c and H_{ex}. Experiment[4] and models[2,3,5] indicate that $H_{ex} \propto J_{ex}\vec{S}_F \cdot \vec{S}_{AF}$, where J_{ex} represents the interfacial exchange coupling (believed to be related to the FM and AF exchange stiffness constants and magnetocrystalline anisotropies) and $\vec{S}_F$ and $\vec{S}_{AF}$ are the interfacial spins in the FM and AF layers, respectively.

There are at least two fundamental parameters that are essential to the temperature evolution of H_{ex} and H_c. The first is the temperature at which the AF spins order, and the second is the cooling field that AF spins are exposed to during the ordering process. To investigate these two parameters, we wish to explore (i) the underlying physics of the AF ordering and cooling fields and (ii) the effect that the FM layer may have on the AF ordering due to its proximity (by providing a local field), and to examine the temperature dependence of H_{ex} and H_c. To enable these studies, we have synthesized pure films of $Ni_{80}Fe_{20}$ (20 nm thick) and Co_3O_4 (15 nm thick), and, using the same deposition conditions, a $Ni_{80}Fe_{20}/Co_3O_4$ film. The Néel temperature (T_N) of bulk Co_3O_4 is 40 K (Ref. 6) and the Curie temperature (T_C) of bulk $Ni_{80}Fe_{20}$ is 800 K,[7] making this $Ni_{80}Fe_{20}/Co_3O_4$ a system with a T_C/T_N that is at least an order of magnitude greater than most other exchange-coupled thin-film systems.[3] With such a significant difference in the energies associated with the FM and AF moment ordering processes, effects of a field, be it from the locally ordered FM or externally applied fields, should clearly impact the AF.

The FM and AF layers are composed of ~10 nm diameter single-domain columns that penetrate the whole film thickness.[8] This nanoscale columnar structured thin-film provides a different interface geometry from the typical textured, multidomain thin film.[2,3] This unusual microstructure leads to an unusual temperature behavior of both H_{ex} and H_c, which suggests that different magnetization reversal mechanisms occur in the left and right branches of the hysteresis loop. Several groups have previously studied this asymmetry of the left and right coercive fields.[9–13] However, the physical mechanism behind the asymmetry of the coercive fields is an open question, and a complete description of the temperature dependence is still lacking. In this paper, we provide a phenomenological description of the temperature dependence of both H_{ex} and H_c that incorporates this asymmetry of the left and right coercive fields.

II. EXPERIMENTAL METHODS

A dual ion-beam deposition technique was used to make the thin film.[14] The system consists of a Kaufman deposition source and End-Hall-assisted source. The Kaufman source is used to focus an argon ion beam onto a target surface (either $Ni_{80}Fe_{20}$ or Co), while the End-Hall source is used to clean or *in situ* bombard the substrate during deposition with an oxygen-argon mixture. This deposition system allows in situ creation of a specific oxide system, and thus we can manufacture the thermodynamically less stable oxides, such as Co_3O_4. A pure 15-nm-thick Co_3O_4 film was deposited on top of a Si(100) substrate, and this sample was used to determine the basic magnetic properties of the thin-film antiferromagnet. To study the effects of exchange coupling with the Co_3O_4, a 15-nm-thick Co_3O_4 film was deposited on top of a Si(100) substrate with a 20 nm $Ni_{80}Fe_{20}$ capping film. No external field was used during deposition. A JEOL (JEM-

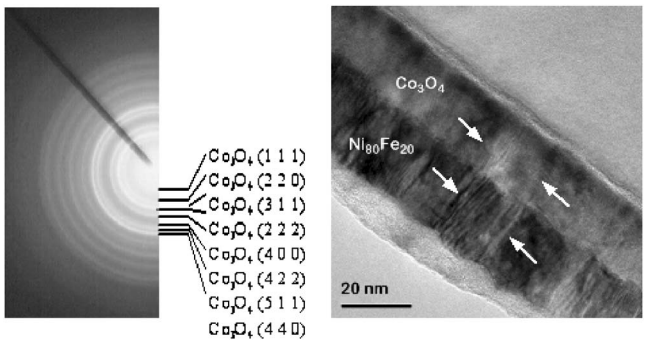

FIG. 1. Transmission electron microscope diffraction pattern of the Co_3O_4 film (left) and cross-sectional view (right) of the $Ni_{80}Fe_{20}/Co_3O_4$ film. Arrows point out the columnar structure in the film components.

2010) transmission electron microscope (TEM) operating at 200 kV was used for microstructural analysis. Magnetic measurements were performed in a Quantum Design magnetometer and susceptometer where the film was field cooled (with the film in the 50 kOe field plane) from 350 K down through the Néel temperature to study exchange bias. The diamagnetic susceptibility of the Si substrate was subtracted from the magnetization data. This high-field susceptibility was used to determine the substrate volume of the sample, and with known substrate and film thicknesses, this information was used to estimate the volume of the $Ni_{80}Fe_{20}/Co_3O_4$ film. ac susceptibility measurements were performed with a 10 Oe drive field at frequencies between 10 and 10 kHz. Zero-field-cooled measurements were performed right after the superconducting solenoid had undergone its initial cooldown from room temperature to ensure that no trapped flux was present while the films were cooled to base temperature.

III. RESULTS AND DISCUSSION

Figure 1 shows a TEM electron-diffraction pattern of the pure Co_3O_4 film. The electron-diffraction pattern uniquely identifies the pure oxide formation of Co_3O_4, a result that has been confirmed using x-ray diffraction.[14] Similar TEM results on the $Ni_{80}Fe_{20}/Co_3O_4$ film show that the microstructure consists of fine equiaxed grains that extend throughout the film thickness, with grain sizes that are ~10 nm, smaller than the film layer thicknesses derived from cross-sectional TEM micrographs. In addition, cross-sectional TEM micrographs, an example of which is in Fig. 1, also show that each layer has a columnar structure that runs perpendicular to the film surface.

The temperature-dependent ac susceptibility (χ_{ac}) of the Co_3O_4 film, shown in Fig. 2, was measured at 1 and 10 kHz. The film was zero-field-cooled (ZFC) to 5 K, and χ_{ac} was measured with heating. The temperature dependence of the real component χ'_{ac} is in good agreement with $\chi(T)$ of bulk Co_3O_4.[6] There is no apparent frequency dependence to $\chi_{ac}(T)$ which is consistent with a magnetic phase transition and not with a dynamical freezing of superparamagnetic, single-domain crystallites. To determine T_N, we use the in-

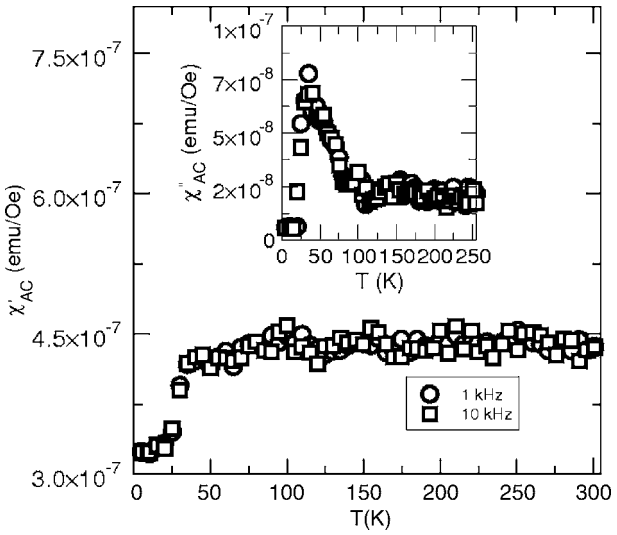

FIG. 2. In-phase component of the ac susceptibility (χ'_{ac}) as a function of temperature for the 15-nm-thick pure Co_3O_4 film. Insets show the out-of-phase component (χ''_{ac}) around T_N.

flection point of $\chi'_{ac}(T)$ [i.e., the maximum of $d\chi'_{ac}(T)/dT$] that marks T_N=35 K, which is also in good agreement with the peak in $\chi''_{ac}(T)$ (Fig. 2, inset). This slightly lower T_N compared to the bulk value of 40 K can be accounted for via the film microstructure. The Co_3O_4 film has a slightly expanded unit cell compared to the bulk, and this weaker interatomic exchange will alter T_N. Assuming that $d(\ln J)/d(\ln V) = -\gamma_m$ ($\gamma_m = \frac{10}{3}$ is an effective magnetic Grüneisen constant) (Ref. 15) provides an estimate of the change in $J \propto T_N$ for a thin film, where V is the change in the unit cell volume and the effective exchange interaction is J.[15] Using $d(\ln J) \approx \ln J_f/J_b$ and $d(\ln V) \approx \ln V_f/V_b$ (f and b represent the film and bulk values), we find for $V_b/V_f = 0.953$ that T_N should be reduced by 5 K from its bulk value, in excellent agreement with our measured film T_N. By contrast, when the AF Co_3O_4 film is coupled to the FM $Ni_{80}Fe_{20}$ film, a similar temperature scan of χ_{ac} (Fig. 3, top panel) presents a very different ordering picture. From 350 to ~250 K there is a gradual increase in χ_{ac} (consistent with Curie-Weiss behavior). However, below 250 K, there is a sudden decrease in $\chi'_{ac}(T)$ that is very similar to that observed around T_N of the pure Co_3O_4 film. Since the $Ni_{80}Fe_{20}$ film component is significantly below its bulk T_C with a constant χ_{ac} (bottom panel of Fig. 3) in this temperature regime, we propose that this Curie-Weiss $\chi'_{ac}(T)$ of the $Ni_{80}Fe_{20}/Co_3O_4$ film is a signature of nascent ordering of AF moments at the interface with their orientation canted toward the FM interface moments. The $Ni_{80}Fe_{20}/Co_3O_4$ film $\chi_{ac}(T)$ has a noticeable frequency dependence until ~150 K, where on further cooling χ_{ac} remains constant, indicating that the moments in the system are static and ordered. Using the same criterion to establish T_N for the Co_3O_4 film, we set $T_N \sim 205$ K by way of the maximum of $d\chi'_{ac}/dT$ that occurs at a similar temperature to the peak in $\chi''_{ac}(T)$. It is also interesting to note that there is a difference in $\chi_{ac}(T)$ when the $Ni_{80}Fe_{20}/Co_3O_4$ system is cooled or heated through its T_N. While the basic temperature evolution of $\chi_{ac}(T)$ is the same (Fig. 4) from 350 to 5 K or

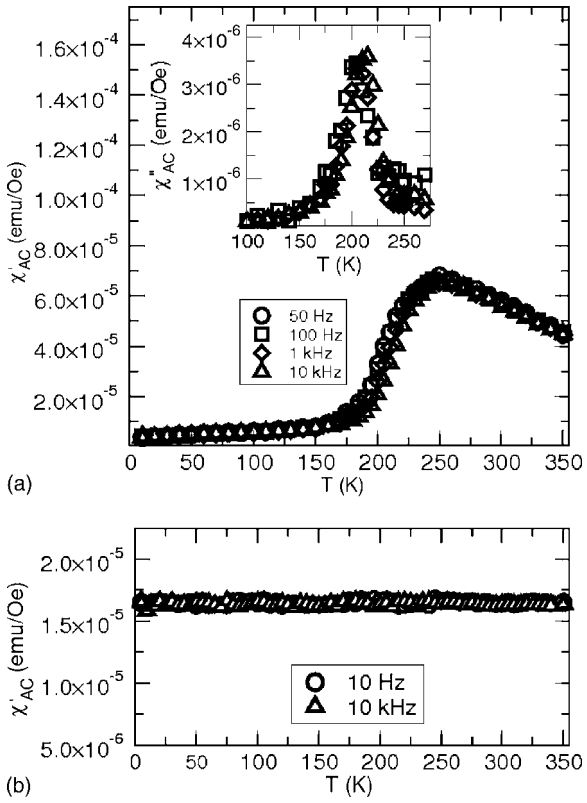

FIG. 3. Top: in-phase component of the ac susceptibility (χ'_{ac}) as a function of temperature for $Ni_{80}Fe_{20}/Co_3O_4$ film. Insets show the out-of-phase component (χ''_{ac}) around T_N. Bottom: in-phase component of the ac susceptibility (χ'_{ac}) as a function of temperature for the 20-nm-thick pure $Ni_{80}Fe_{20}$.

from 5 to 350 K, the magnitudes of χ'_{ac} and χ''_{ac} are larger when the system is cooled through T_N than when the film is heated through T_N. We propose that this behavior is another signature of the effects of the Co_3O_4 interface moments be-

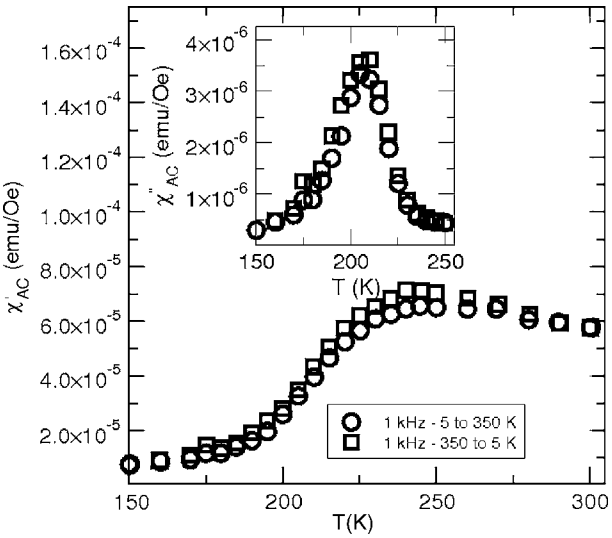

FIG. 4. In-phase component of the ac susceptibility (χ'_{ac}) for the $Ni_{80}Fe_{20}/Co_3O_4$ film as a function of increasing temperature (○) and decreasing temperature (□). Insets show the out-of-phase component (χ''_{ac}) around T_N.

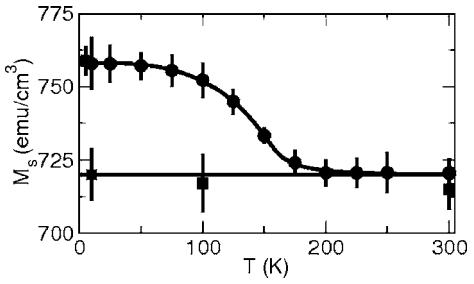

FIG. 5. The temperature dependence of the saturation magnetization (M_s) of the film (● are $Ni_{80}Fe_{20}/Co_3O_4$ results and ■ are pure $Ni_{80}Fe_{20}$ film results). Solid lines are fits described in the text.

ing exchange coupled to the interface moments of the $Ni_{80}Fe_{20}$. With cooling from above T_N, the local field provided by the FM $Ni_{80}Fe_{20}$ enables Co_3O_4 interface moments to cant toward the FM layer, yielding a larger χ_{ac} that results from these canted moments ordering around this temperature. Further cooling fixes the Co_3O_4 moment orientation further into the bulk of this film, eventually locking all moments into a static, ordered configuration at the lowest temperatures. At low temperatures, the moment configurations through the bulk of both film components (as well as the interface) are firmly established, and with warming toward and through T_N, the effects of the FM on the AF interface moments will be reduced as the Co_3O_4 moments in the bulk of this film component will still be ordered, and the interface Co_3O_4 moments will not be as easily rotated toward the orientation of the FM $Ni_{80}Fe_{20}$ moments, resulting in a smaller χ_{ac} signal. Further evidence of magnetic ordering of the AF at an elevated temperature is provided by the temperature dependence of the measured saturation magnetization (M_s) of the $Ni_{80}Fe_{20}/Co_3O_4$ film, shown in Fig. 5. From 350 down to ~205 K, M_s is constant, consistent with the FM component below T_C. At approximately 205 K, M_s increases from ~720 emu/cm^3 to a constant $M_s \sim 760$ emu/cm^3 that is reached below 50 K. The change $\Delta M_s(T)$ is well described by a Brillouin function that incorporates the presence of a small field. The requirement of this small field to correctly describe $\Delta M_s(T)$ is consistent with the picture of the FM layer providing a local-field environment that affects the Co_3O_4 interface moments as they undergo local ordering. The onset temperature is in good agreement with the increase in χ_{ac} (Fig. 3) that measures the larger moment fluctuations and concomitant dissipative losses that occur during a magnetic phase transition. The AF "order" near the interface likely occurs in a canted configuration with moments pointing toward the FM layer, instead of the usual second nearest-neighbor superexchange coupled spin configuration with spins in opposite directions as in pure Co_3O_4.[6] With cooling, the gradual increase of M_s is likely due to this canted order percolating into the bulk of the AF component, with the canting angle decreasing into the AF film. At a temperature around 50 K, $M_s(T)$ is essentially constant, and the usual staggered magnetization configuration of the AF has been achieved deeper into the bulk of the Co_3O_4.

At temperatures above the peak in $\chi''_{ac}(T)$, hysteresis loops describe the magnetism of the $Ni_{80}Fe_{20}$ film layer, where the

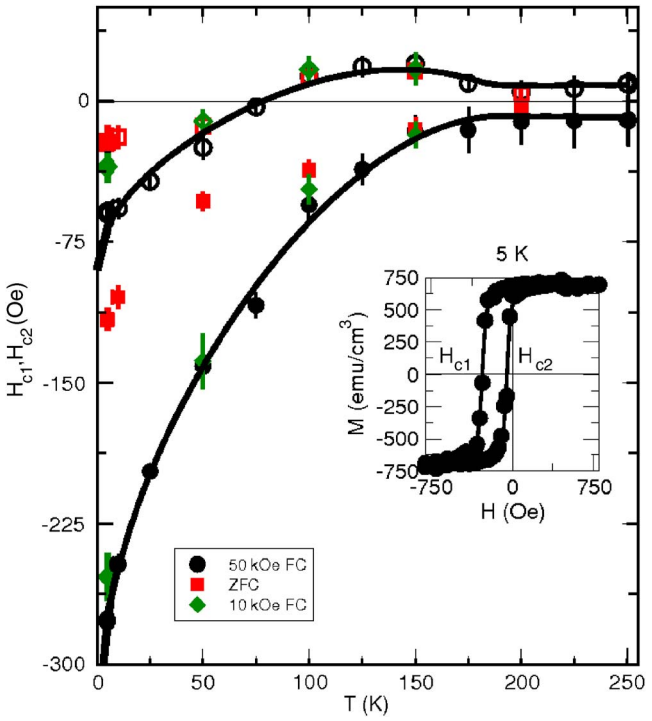

FIG. 6. (Color online) Temperature dependence of H_{c1} (lower curve) and H_{c2} (upper curve). ● are 50 kOe field-cooled results, ◆ are 10 kOe field-cooled results, and ■ are zero-field-cooled results for the $Ni_{80}Fe_{20}/Co_3O_4$ thin-film. The inset shows a typical hysteresis loop after having been field cooled in 50 kOe.

left coercive field H_{c1} and the right coercive field H_{c2} are symmetric about the magnetization axis and temperature independent (Fig. 6). At temperatures significantly below the peak in $\chi''_{ac}(T)$, the effects of exchange coupling are easily observable, as shown by the typical hysteresis loop in the inset to Fig. 6, with H_{c1} and H_{c2} offset by the exchange bias loop shift, $H_{ex}=(H_{c1}+H_{c2})/2$. Note that in the range of temperatures between 150 and 200 K (Fig. 6), there is no loop shift but rather a temperature dependence of both H_{c1} and H_{c2}, which corresponds to an enhanced coercivity $H_c=(H_{c2}-H_{c1})/2$ compared to temperatures both above the peak in $\chi''_{ac}(T)$ and above the increase in $M_s(T)$. Below 150 K, the hysteresis loop is shifted, indicating that exchange bias is present and this behavior identifies the temperature for the onset of the exchange bias to be $T_{ex}=150\pm5$ K. T_{ex} is independent of whether the film was prepared in a field-cooled or zero field-cooled configuration (Fig. 6), evidence that the local field provided by the $Ni_{80}Fe_{20}$ is responsible for the enhanced T_N and not an external field.

We interpret the increase in coercivity and the frequency dependence of $\chi_{ac}(T)$ in the temperature range of 150–205 K to be from a distribution of grain sizes in the AF. This would result in a distribution of blocking temperatures in this same range and could lead to an asymmetry in $H_{c1}(T)$ and $H_{c2}(T)$ and different magnetization reversal mechanisms at these fields.[9] The combination of the proximity enhanced T_N and the nanocolumnar microstructure of the film components results in an unusual temperature dependence of H_{c1} and H_{c2}. In order to interpret the temperature dependence of both, we have used the following form for the left and right coercive fields which correspond to thermal fluctuations over an energy barrier,[16]

$$H_{c1}(T) = A(1 - \sqrt{T/T_1}) - C\Delta m_s(T),$$

$$H_{c2}(T) = B(1 - \sqrt{T/T_2}) + C\Delta m_s(T), \quad (1)$$

where A and B are constants that allow for different reversal mechanisms when switching the sign of the applied field and the last term describes the enhanced coercivity in the temperature range between 150 and 205 K which is assumed to be proportional to the change in the reduced magnetization, $\Delta m_s(T)=\Delta M_s(T)/\Delta M_s(0)$. The enhanced coercivity is due to an effective anisotropy field, resulting from the canting of the AF spins near the interface. A fit using Eq. (1) to the 50 kOe data is shown by the solid lines in Fig. 6, where $A=-392\pm20$ Oe, $B=-160\pm12$ Oe, $T_1=166\pm17$ K, $T_2=179\pm10$ K, and $C=60\pm8$ Oe. The temperatures T_1 and T_2 represent average blocking temperatures for the two coercive fields and are roughly midway between $T_{ex}=150$ K and $T_N=205$ K.

The temperature dependence of H_{c1} and H_{c2} displayed in Fig. 6 is well described by Eq. (1) and, to our knowledge, cannot be predicted either by current models of exchange bias or by asymmetric magnetization reversal mechanisms.[2,9–13] At high temperatures (from 300 to ~205 K), the term $C\Delta m_s(T)$ is small and independent of temperature leading to a small and temperature-independent coercivity in the $Ni_{80}Fe_{20}/Co_3O_4$ film. The spins in the AF are fluctuating and are responsible for the ac effects in the susceptibility. At intermediate temperatures between ~205 K and 100 K, the interface anisotropy field described by $C\Delta m_s(T)$ is enhanced by the interfacial ordering of the AF Co_3O_4 moments and this is reflected in an enhanced coercivity in this temperature range. At the same time, there is an asymmetry in the behavior of H_{c1} and H_{c2} which results in a measurable exchange bias field. The upper coercive field $H_{c2}(T)$ displays an unusual behavior in this range of temperature. It becomes more positive with decreasing temperature before taking on negative values. That is, the hysteresis loop is becoming wider as it shifts along the negative field axis. For temperatures below 100 K, the effective anisotropy field $C\Delta m_s(T)$ is once again essentially temperature independent and the exchange coupling between the $Ni_{80}Fe_{20}$ and Co_3O_4 nanocolumns is firmly established. In this region, the temperature dependences of H_{c1} and of H_{c2} are both dominated by the dynamical freezing of the AF grains. Figure 7 shows the same data as in Fig. 6 in terms of $H_{ex}(T)$ and $H_c(T)$. The exchange bias clearly appears at a temperature below that where the coercivity becomes enhanced. This behavior also occurs when the film is prepared in a zero-field-cooled state and indicates that the local field that enables the enhanced T_N is providing an environment where the AF interface moments order in a canted orientation and basically lock in with the FM interface moments.

Exchange bias can also occur between a magnetically soft system such as $Ni_{80}Fe_{20}$ and a magnetically hard FM material.[2,3] The magnetic signature of this situation is a

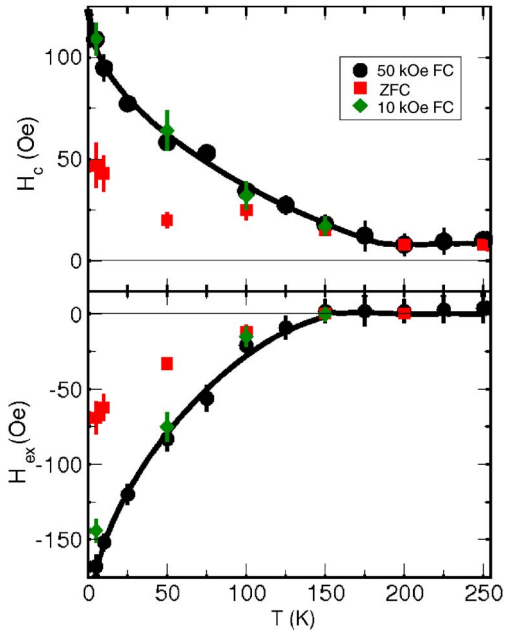

FIG. 7. (Color online) Exchange bias loop shift H_{ex} (lower panel) and coercivity H_c (upper panel) as a function of temperature for the $Ni_{80}Fe_{20}/Co_3O_4$ thin film. The ● are 50 kOe field-cooled results, ◆ are 10 kOe field-cooled results, and ■ are zero-field-cooled results. Solid lines were obtained from the fits to $H_{c1}(T)$ and $H_{c2}(T)$ using Eq. (1).

temperature-dependent shift of the hysteresis loop along the magnetization axis. We can rule out this scenario in the $Ni_{80}Fe_{20}/Co_3O_4$ film by way of local compositional and structural characterization done with TEM (Ref. 14) in addition to there being no measured shift of the hysteresis loops along the magnetization axis. Exchange bias in the $Ni_{80}Fe_{20}/Co_3O_4$ film is clearly occurring in a FM/AF system with significantly enhanced T_N enabled by proximity effects due to the FM.

An ~10% increase of T_N in an AF NiF_2-based thin-film system[15] has been recently observed. The origin of the increase in T_N was attributed to lattice mismatch strain between the NiF_2 and MgF_2,[15] similar to the origin of the decreased T_N in our Co_3O_4 film (see above). However, lattice mismatch strain cannot be the reason behind the enhanced T_N we observe in the $Ni_{80}Fe_{20}/Co_3O_4$ film, since this would require a reduction in the unit cell volume, which is inconsistent with x-ray and TEM diffraction results that measure an expanded unit cell (above). Neutron-diffraction studies have established that T_N in a FM/AF bilayer can be increased by proximity to the FM, with an ~50% increase of T_N in a Fe_3O_4/CoO thin-film system.[17] Furthermore, recent theoretical calculations[18] of AF/FM thin-film bilayers indicate that the subsystem with the larger ordering temperature induces magnetic order into the other one. A similar physical mechanism is likely responsible for this large increase in T_N in this $Ni_{80}Fe_{20}/Co_3O_4$ thin-film system.

IV. CONCLUSIONS

In summary, exchange bias is established even when the thin film is zero-field-cooled, and its temperature dependence is dominated by the thermal fluctuations of the single-domain nanocolumns that make up its microstructure. Both $H_{c1}(T)$ and $H_{c2}(T)$ exhibit thermally driven magnetism but with different energy barriers or different domain wall reversal mechanisms during positive-to-negative and negative-to-positive field sweeps. Field cooling the film sets a significantly stronger exchange coupling between the FM and AF moments at the interface. Most interesting is the atypical enhancement of the AF ordering temperature that is consistent with surface AF moments ordering at the FM/AF interface, where the interaction energy between moments near the interface seems to be significantly larger than that in the bulk. We are currently investigating possible origins of this unusual magnetism by way of experiments that probe the local interface magnetism as well as by Monte Carlo simulations.

ACKNOWLEDGMENTS

This work was supported by the Natural Sciences and Engineering Research Council of Canada and in part by the National Science Council of Taiwan.

[1] W. H. Meiklejohn and C. P. Bean, Phys. Rev. **105**, 904 (1957).
[2] J. Nogués and I. K. Schuller, J. Magn. Magn. Mater. **192**, 203 (1999).
[3] A. E. Berkowitz and K. Takano, J. Magn. Magn. Mater. **200**, 552 (1999).
[4] S. Roy, M. R. Fitzsimmons, S. Park, M. Dorn, O. Petracic, I. V. Roshchin, Z.-P. Li, X. Batlle, R. Morales, A. Misra *et al.*, Phys. Rev. Lett. **95**, 047201 (2005).
[5] A. P. Malozemoff, Phys. Rev. B **37**, 7673 (1988).
[6] W. L. Roth, J. Phys. Chem. Solids **25**, 1 (1974).
[7] R. C. O'Handley, *Modern Magnetic Materials, Principles and Applications* (Wiley, New York, 2000).
[8] J. van Lierop, K.-W. Lin, Z.-Y. Guo, and B. W. Southern, J. Appl. Phys. **99**, 08C101 (2006).
[9] T. Gredig, I. N. Krivorotov, P. Eames, and E. D. Dahlberg, Appl. Phys. Lett. **81**, 1270 (2002).
[10] M. R. Fitzsimmons, P. Yashar, C. Leighton, I. K. Schuller, J. Nogués, C. F. Majkrzak, and J. A. Dura, Phys. Rev. Lett. **84**, 3986 (2000).
[11] B. Beckmann, U. Nowak, and K. D. Usadel, Phys. Rev. Lett. **91**, 187201 (2003).
[12] Z.-P. Li, O. Petracic, R. Morales, J. Olamit, X. Batlle, K. Liu, and I. K. Schuller, Phys. Rev. Lett. **96**, 217205 (2006).
[13] I. K. Schuller, MRS Bull. **9**, 642 (2004).
[14] K.-W. Lin, F.-T. Lin, Y.-M. Tzeng, and Z.-Y. Guo, Eur. Phys. J. B **45**, 237 (2005).

[15] H. Shi, D. Lederman, K. V. O'Donovan, and J. A. Borchers, Phys. Rev. B **69**, 214416 (2004).
[16] I. S. Jacobs and C. P. Bean, in *Magnetism*, edited by G. T. Rado and H. Shul (Academic, New York, 1963), Vol. III, p. 271.
[17] P. J. van der Zaag, Y. Ijiri, J. A. Borchers, L. F. Feiner, R. M. Wolf, J. M. Gaines, R. W. Erwin, and M. A. Verheijen, Phys. Rev. Lett. **84**, 6102 (2000).
[18] P. J. Jensen, H. Dreyssé, and M. Kiwi, Eur. Phys. J. B **46**, 541 (2005).